

## LIFETIME OF THE MUON

This experiment allows the measurement of the mean lifetime of the muon ( $\mu$ ) using contemporary instrumentation and experimental techniques. The muon was discovered by J. C. Street and E. C. Stevenson at Harvard University and almost simultaneously at Caltech by C.D. Anderson and S. H. Neddermeyer in 1937 [See *Phys Rev*, **51**, 884 (1937)]. The subsequent work here of Millikan, Anderson, Neddermeyer, Neher, Stever, Leighton, et al, during the decade preceding, and the years immediately following World War II helped establish the foundations of cosmic-ray physics. Natural muons continue to be of interest in many areas of physics, while the production of intense beams of the artificial variety at various "meson factories", permits exploiting the muon's large magnetic moment, violation of parity, and unique ability to closely approach nuclei, and to develop the muon spin relaxation techniques that provide for an exceptional sensitivity in investigating the structure of materials.

The intent of this experiment is to determine the distribution of time intervals between the entry of a muon into a scintillator (in which the muon stops) and its subsequent decay. A fit of the distribution to  $\exp(-t/\tau)$  then gives the lifetime  $\tau$ .

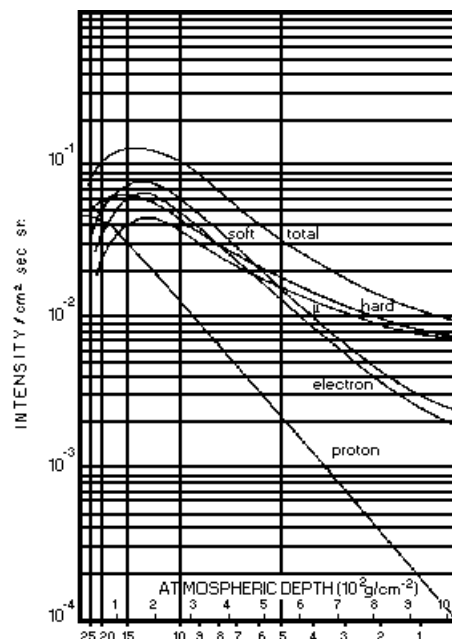


Figure 1. Components of cosmic-ray flux. ~80% of the "cosmic rays" at sea level are muons, the remainder electrons plus a lesser number of protons. The flux in our laboratory is  $\approx 10^{-2} \text{ cm}^{-2} \text{ s}^{-1} \text{ sr}^{-1}$ .

## ORIGIN OF MUONS:

Cosmic-ray muons are produced by the interaction of extra-terrestrial particles (primaries) with the Earth's upper atmosphere. Cosmic rays detected at the Earth's surface are a mixture of energetic primaries and secondaries (hard component) and lower energy secondaries (soft component). The primary flux consists of the extremely high energy ( $>10^9$  eV) protons,  $\alpha$ -particles, and a few light nuclei. Interactions with the upper atmosphere produces a secondary flux of protons, neutrons, and two forms of  $\pi$  mesons (neutral and charged). Neutral  $\pi$  mesons decay quickly into photons that multiply into showers, while the charged  $\pi$  mesons decay to muons plus neutrinos. Muons (+ or -) carry the same charge as an electron, with a mass 206.8 times larger. Their kinetic energy is from zero to many GeV, they have a spin of 1/2, and a magnetic dipole moment 3.18 times that of the proton. The  $\mu^-$  disappears in either of two ways; capture by a nucleus, with the emission of a neutrino and a neutron, or by spontaneous decay to an electron and neutrino-anti-neutrino pair after coming to rest:  $\mu^- \rightarrow e^- + \nu_e + \bar{\nu}_\mu$ . The probability of capture by a nucleus is small for low Z materials but increases rapidly with increasing Z. The  $\mu^+$ , strongly repulsed by nuclei, have only the decay path:  $\mu^+ \rightarrow e^+ + \nu_e + \bar{\nu}_\mu$ . Energy losses are by ionization until they come to rest. The subsequent decay-electron spectrum is a continuum with a shape similar to a  $\beta$ -spectrum, with an energy range from near zero to an end point of about 53 MeV. While the lifetimes for a  $\mu^+$  and a  $\mu^-$  are the same (2.1970  $\mu$ s), the measured mean lifetime in matter becomes shorter for the  $\mu^-$  with increasing Z because of the competing capture by nuclei. Lifetime measurement must be examined carefully since it will most probably be a composite value for the lifetimes of both  $\mu^+$  and  $\mu^-$ .

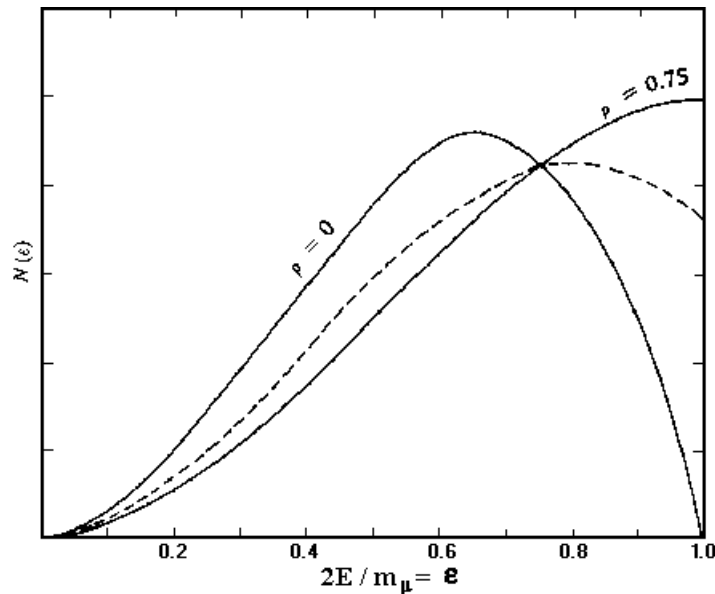


Figure 2. Energy spectrum of muon decay electrons.

References: (4) Chap. 1, (2) p. 730-747, (1) p. 633--640 .

# INTERACTIONS BETWEEN CHARGED PARTICLES AND MATTER

The fundamental mechanism for detecting ionizing radiation is the transfer of energy from radiation to an appropriate material. The character of the radiation and its energy range determine the exact process(es) involved.

This experiment requires the detection of muons and electrons ( $E < 53 \text{ MeV}$ ).

Energetic particles (muons and electrons) lose energy to matter by Coulomb interactions between the particles and the atomic electrons, and to some extent, nuclei. Electrons typically gain enough energy to escape from their parent atoms. The principal processes for energy loss are:

- **Inelastic collisions** - with energy transferred to electrons of the material (ionization). **Primary mechanism for electrons, beta-rays, and muons.**
- **Bremsstrahlung** - emission of electromagnetic radiation by the decelerating particle. **Principal source of energy loss for relativistic particles  $E \gg mc^2$ .** *Of minimal importance for muons because of their large mass.*

Like electrons, muons are capable of transferring energy only by the electromagnetic and weak interactions, with the rate of energy loss determined by the initial energy and the  $Z$  of the material. The rate ( $dE/dX$ ) drops slowly with decreasing energy to a minimum ("Minimum Ionizing"), then rises again at low energies. The Bethe formula for particles is:

$$\frac{dE_q}{dX} = 4\pi NZ \frac{z^2 e^4}{mv^2} \left[ \ln \left( \frac{2\gamma^2 mv^2}{\hbar\omega} \right) - \frac{v^2}{c^2} \right] .$$

Here  $m$  is the electron mass, so that  $dE/dX$  depends only on the charge  $z$  and velocity  $v$  of the particle. The correction for density effects is:

$$\lim_{\beta \rightarrow 1} \Delta \left( \frac{dE}{dX} \right) = \frac{(ze)^2 \omega_p^2}{c^2} \left[ \ln \left( \frac{\gamma \omega_p}{\omega} \right) - \frac{1}{2} \right] .$$

The "universal" value of  $dE/dX$  for "minimum ionizing" particles is:  **$dE/dX \approx 2 \text{ MeV}/(\text{gm}/\text{cm}^2)$ .**

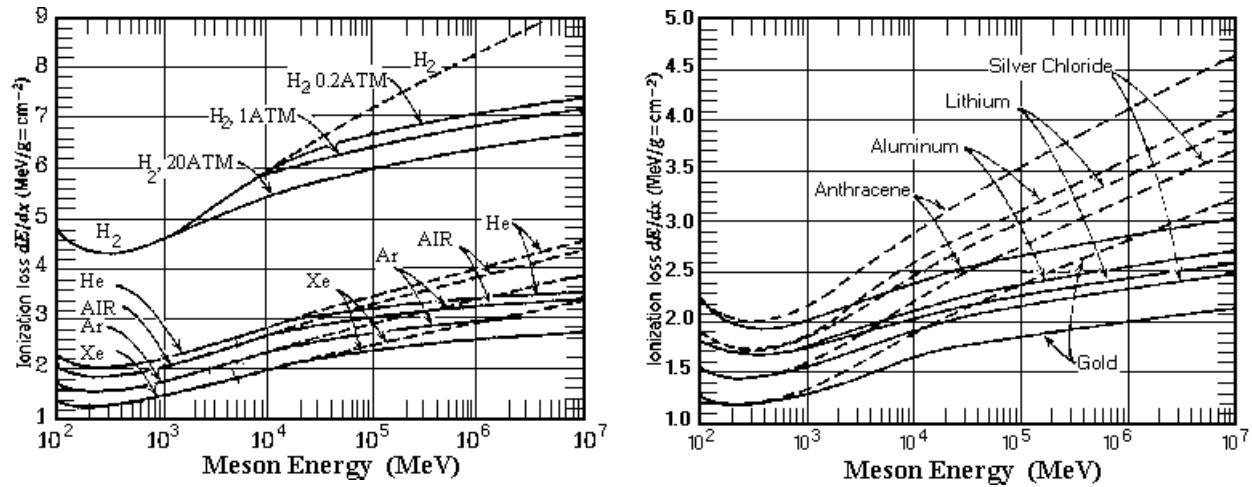


Figure 3. Energy loss for muons in gases and solids, ---- = losses if the density effect is ignored.

References:(4) Chap.2, (3) p. 11-141, (5) p. 626-637 .

## THE SCINTILLATION MECHANISM:

Charged particles transfer energy to matter, either by generating heat, or raising electrons to excited states. If the material is a scintillator, when these electrons decay to lower-energy states some of their excess energy is carried off by a photon in the short blue to long UV regions of the spectrum.

Photon production in organic scintillators is a molecular process conveniently described by the potential energy diagram of Fig. 4. The lower curve represents the potential energy when all of the electrons are in their ground states; the upper curve showing the potential energy of an excited state. The Franck-Condon principle states that any energy deposited not dissipated as heat will cause a transition from  $A_0$  to  $A_1$  ( $E_e = E_{A1} - E_{A0}$ ) in a time ( $\sim 10^{-13}$  s) that is short compared to the vibration time of the molecule. Lattice vibrations produce an energy loss that moves the molecule to  $B_1$ . After a time ( $\sim 10^{-8}$  s) that is long compared to the vibration time, the excited state decays to the ground state ( $B_1$  to  $B_0$ ), with excess energy ( $E_p = E_{B1} - E_{B0}$ ) producing a photon. *This process produces about 1 photon per 100 eV of energy deposited and is called fluorescent emission.* Because the energy required to produce an excited state ( $E_e$ ) exceeds that carried away by an emitted photon ( $E_p$ ), the probability that the emitted photon will be re-absorbed is negligible, with the result that the scintillator is transparent to the light it generates.

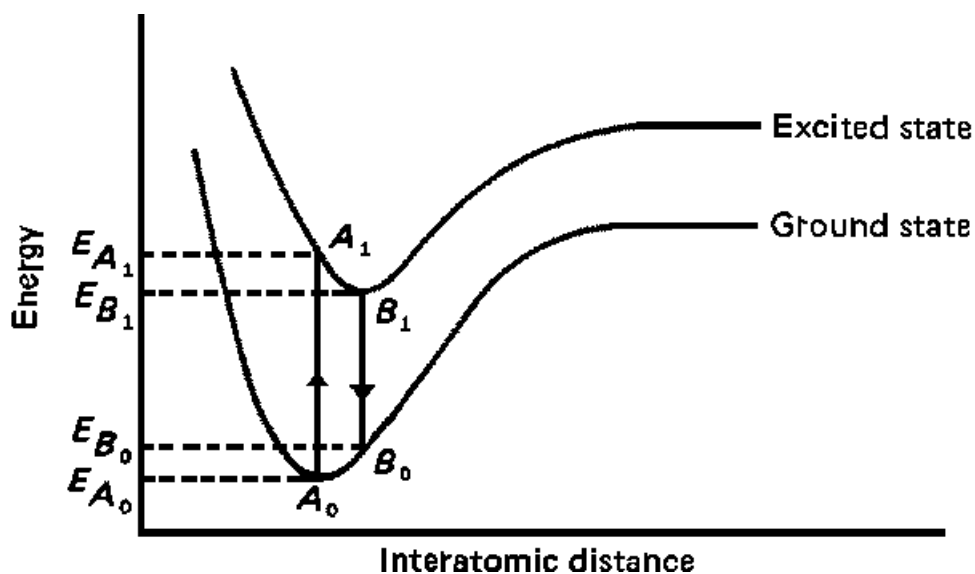


Figure 4. Energy diagram (simplified) of an organic scintillator.

Secondary scintillators are frequently added to "shift" the emitted photons to longer wavelengths to more closely match the peak of PMT photocathode spectral response curves. These fluors exhibit high absorption at the wavelength of the photons generated by the primary scintillator. They respond to the energy carried by the primary photons in exactly the same manner as above, except that all energy levels are lower.

References: (4) p. 201 - 204.

## EQUIPMENT AND EXPERIMENTAL TECHNIQUES

### DETECTOR:

The 0.21 m<sup>3</sup> of liquid scintillator mixture consists of a light oil carrier (primary solvent), a primary scintillator, a secondary solvent and a secondary wavelength-shifting fluor in a titanium dioxide-lined container. A "collector bar", on the container axis, contains a third wavelength shifter (BBQ), that efficiently absorbs photons produced by the secondary fluor to then emit at a longer wavelength that matches the peak spectral sensitivity of the photomultiplier.

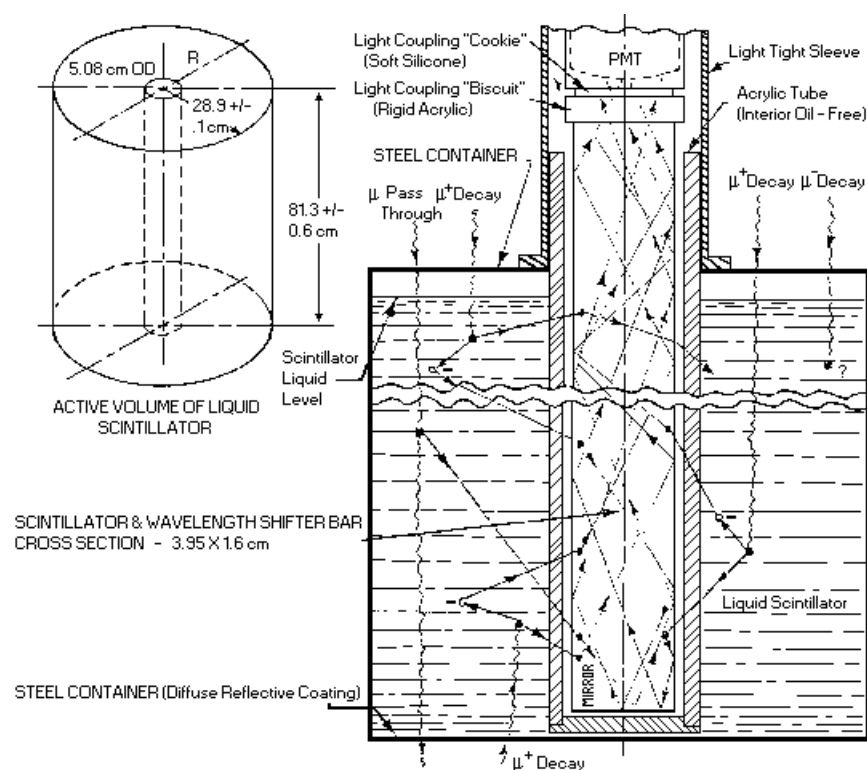


Figure 5. Details of the scintillator container and light collection structure.

Photons generated in the shifter bar are directed towards the PMT by total internal reflections, assisted by a mirror cemented at the bottom. A UV-transparent tube isolates the collector/shifter bar from the oil to permit total internal reflections by maximizing the change in index of refraction at the interface between the air and the highly polished surface of the bar.

Relevant parameters for the liquid components are:

- \*\* Primary Solvent/Carrier - light mineral oil.
- \*\* Index of refraction - 1.47.
- \*\* Attenuation length ( $l/e$ ) > 3 m.
- \*\* Primary fluor - PPO, 2.3 g/l of primary solvent.
- \*\* Wavelength of maximum emission - 360 nm.
- \*\* Decay time - 1.6 ns.
- \*\* Secondary solvent - Cyclosol 53, 50 ml/l of primary solvent.
- \*\* Secondary fluor - Bis-MSB, 20 mg/l.
- \*\* Wavelength of maximum emission - 420 nm.
- \*\* Decay time - 1.35 ns.
- \*\* Density of mixture -  $0.858 \text{ g/cm}^3$ .
- \*\* H atoms/ $\text{cm}^3$  -  $6.6 \times 10^{22}$

\*\* C atoms/cm<sup>3</sup> -  $3.8 \times 10^{22}$

\*\* Ratio H/C - 1.7

\*\* No. Electrons/cm<sup>3</sup> -  $2.96 \times 10^{23}$

Relevant parameters for the collector/shifter bar component are:

\*\* Carrier - acrylic polymer.

\*\* Dimensions - 3.95 cm x 1.6 cm cross section.

\*\* Density - 1.18 g/cm<sup>3</sup>.

\*\* Index of refraction - 1.49.

\*\* BBQ concentration - 90 mg/l of acrylic monomer.

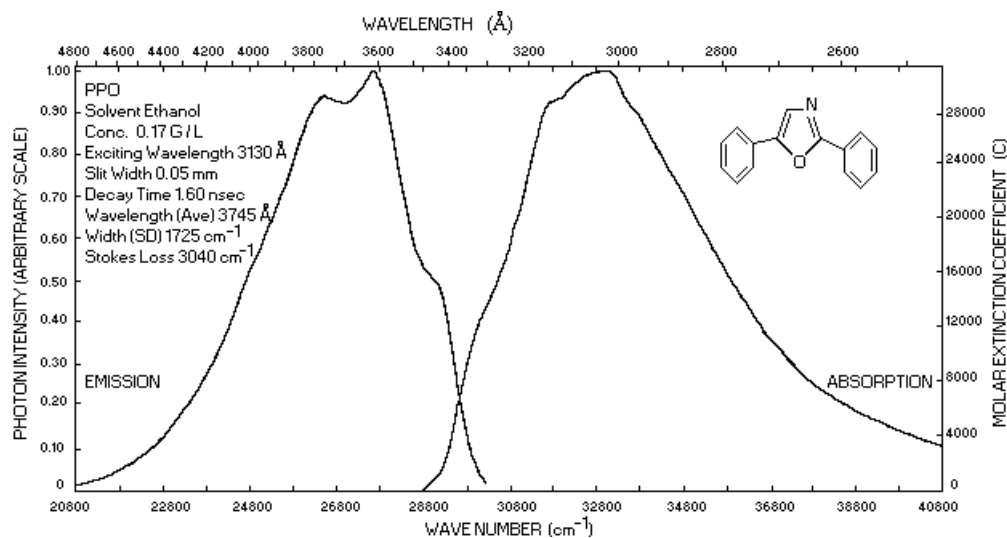
\*\* Wavelength of maximum absorption - < 430 nm.

\*\* Wavelength of maximum emission - 500 (460 to 550) nm.

\*\* Decay time - 25 ns.

\*\* Attenuation length (1/e) - 13.4 mm @ 430 nm,  
3 m @ 500 nm, (5 m with end mirror).

Reference: B. Barish et al, IEEE Transactions on Nuclear Science, (532-536), 1978.



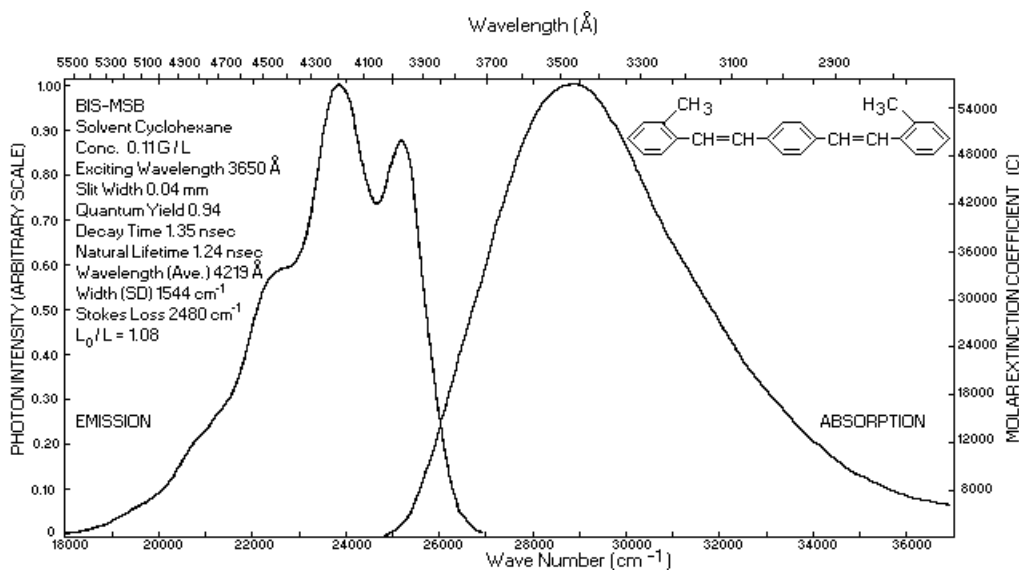


Figure 6. Characteristic emission/absorption spectra for the liquid scintillator components.

Similar curves for the BBQ shifter bar will be peaked at 430 nm for absorption, and 500 nm for emission.

## ELECTRONICS COMPONENTS :

The electronics system is not complicated, but each component must be properly adjusted in the correct order if valid results are to be obtained. Study of the material below, as well as Instruction Manuals, and a review of Experiments 12 and 13 will be essential.

### PHOTOMULTIPLIER:

The 10-stage photomultiplier (RCA type 6655A) is operated at +950 V and feeds a conventional inverting charge-sensitive preamplifier. The relatively slow decay time of the wavelength-shifting scintillator (25 ns) allows use of the preamp and operation of the PMT at a modest voltage, providing the benefits of a very wide dynamic range and a low noise level (dark current). The preamplifier power is derived from the PMT HV divider current.

### SHAPING AMPLIFIER:

The EG&G Ortec Model 474 Timing Filter Amplifier allows optimizing the output pulse width by independent adjustments for the time constants for Differentiation (20 ns to 500 ns) and Integration (10 ns to 500 ns). Note that



simple RC networks are used for pulse shaping (DIFFerentiation and INTEGration), hence **the panel labels describe the RC time constant selected and NOT the actual pulse width**. Note also that the amplitude of the output pulse changes when either parameter is altered. Gain can be varied between 2x and 250x, with a linear output of  $\pm 5$  V into a 50  $\Omega$  load. This amplifier's very fast time response (large bandwidth) requires that its output **MUST ALWAYS** be terminated with 50  $\Omega$ . Failure to do so produces severe reflections and gross

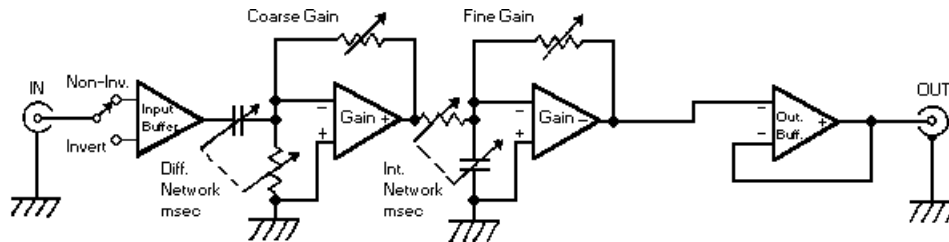


Figure 7. Functional block diagram of EG&G Ortec 474 Amplifier.

non-linearities. Normal operating parameters are with time constants set for 500 ns (DIFF.) and 20 ns (INTEG.), and total GAIN set for either 250x or 2x. **CAUTION:** The OUTPUT polarity switch handle **MUST** be pulled out before attempting to change its position. It is set to NON-INVERTing to produce positive unipolar output pulses suitable for the Gate & Stretcher, or to INVERTing to properly serve the Discriminator.

## LINEAR GATE AND STRETCHER:

The Canberra 1454 Linear Gate and Stretcher accepts narrow **positive-only** inputs between 0.1 V and 10 V amplitude, senses the peak height and stretches the pulse to a width (1 to 5 ms) required by a conventional MCA. Basic gain is 1, but the output may be set to 10, 5 or 3 V full scale, with either polarity (+ **output only for driving the MCA**). The unit's integral non-linearity is < 0.1% of FS. The input network for the fixed Lower Level Discriminator and internal Base Line Restorer (BLR) may be selected for optimal response for three

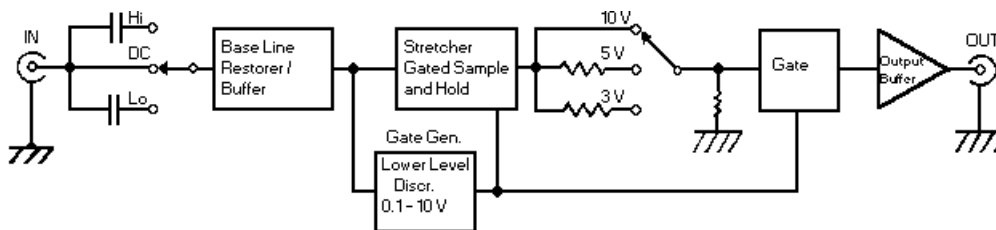


Figure 8. Functional block diagram of Canberra 1454 Gate and Stretcher.

situations: DC for input pulses from amplifiers that have their own BLR facilities, LO is for AC coupled signals with duty cycles of < 20%, and HI is for duty cycles > 20%. For this experiment use the DC position for best results. The GATE switch should be set to ANTI. The MCA Input coupling switch (Rear Panel) must be in the DC position for best results.

## DISCRIMINATOR (DISC.):

The LeCroy Model 821 Quad Discriminator module produces negative "Fast NIM" logic signals when a negative analog input pulse exceeds the Threshold amplitude set by the user. As with all "Fast NIM" electronic modules, the input impedance is  $50\ \Omega$ . The input threshold is  $-0.03$  to  $-1.0\ \text{V}$  (a dynamic range  $> 33:1$ ) set by means of a front-panel screwdriver adjustment (THR). A DC level,  $10\times$  the actual THRESHOLD setting may be measured ( $\pm 5\%$ ) at the front panel THR jack.

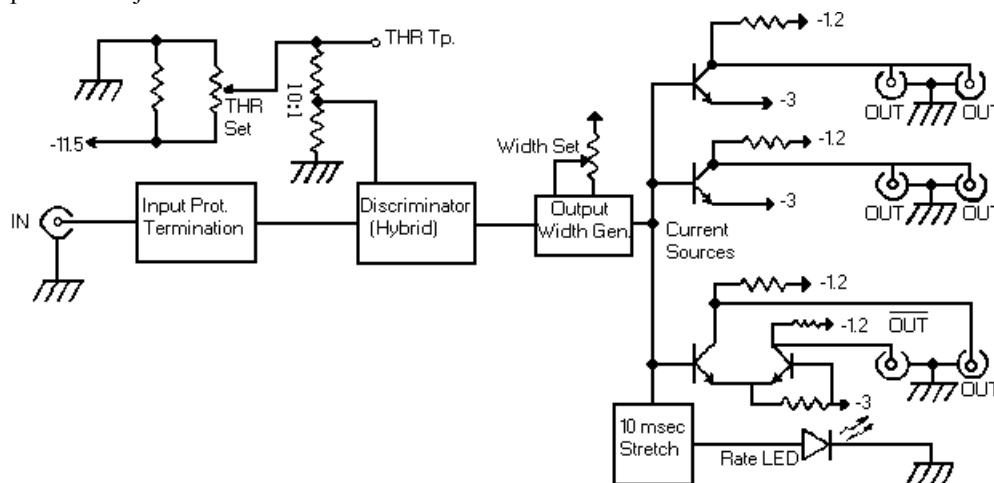


Figure 9. Block diagram of one channel of the LeCroy 821 Quad Discriminator.

Input amplitudes exceeding the  $-1\ \text{V}$  maximum threshold sensing level (safe up to  $\sim -5\ \text{V}$ ) are processed normally (input clamping occurs at  $+1\ \text{V}$  and  $-7\ \text{V}$ ). Just to the right of the THR jack is the RATE Light Emitting Diode (LED) that indicates the presence of output pulses "stretched" to  $10\ \text{ms}$  width to make narrow output pulses "visible" to the MCA. Outputs are produced at the point on the leading edge where the input pulse crosses the Threshold amplitude setting. Input/output delay is typically  $9.5\ \text{ns}$ .

Three independent parallel drivers produce time-coincident outputs at six sub-miniature Lemo panel connectors. Each driver feeds two connectors. The two upper rows of output connectors have a line between parallel connected pairs and provide Negative going signals. (*Significant changes in amplitude and pulse shape occur if parallel outputs are simultaneously loaded.* See remarks under EXPERIMENTAL TASKS.) The lowest connector pair set provides one normal Negative going signal and one complementary Positive transition. Output signals are  $-1.6\ \text{V}$  ( $32\ \text{mA}$ ) into  $50\ \Omega$  with  $5\ \text{ns}$  to  $1\ \mu\text{sec}$  width (normal setting is  $20\ \text{ns}$ ). The INPUT/OUTPUT connectors on this module are sub-miniature push-pull Lemo coaxial types. **CAUTION** - Handle the Lemo connectors with care - the cables are easily destroyed. To remove a cable, always **grasp the knurled sleeve** close to the panel - NEVER THE CABLE - and gently squeeze the connector free, then pull straight out. When inserting a cable push gently in until you hear, or feel, a click.

## TIME-TO-AMPLITUDE CONVERTER (TAC):

The Tennelec 861A Time-to-Amplitude-Converter generates a positive output pulse that has a peak amplitude (+10 V full scale) that is accurately proportional to the time interval between two negative Fast NIM input pulses.

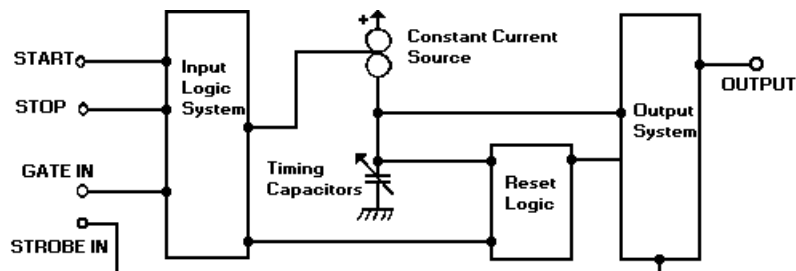


Figure 10. Block diagram of the Tennelec 861A Time-To-Amplitude Converter.

Full-scale times from 50 ns to 200  $\mu$ s are selected with a front-panel switch, with a time-interval resolution of 10 ps (FWHM) on the 50 ns range, and  $< 0.01\%$  on the others. Temperature drift is  $< 10$  ps/ $^{\circ}$ C on the 50 ns range, and  $< 0.015\%$  on all higher ranges. The START/STOP input pulses must meet the NIM standard for Negative Logic Signals, i.e., 3 ns minimum width and  $> 250$  mV minimum amplitude. The 50  $\Omega$  inputs are protected against overloads up to 100 V. The output pulse width may be adjusted between 0.5 to 5  $\mu$ s (normal setting 1.5  $\mu$ s). The integral nonlinearity of the output system is  $< 0.1\%$  from 15 to 200  $\mu$ s, with a differential nonlinearity of  $< 1\%$ . (The Input coupling switch on the TN-7200 MCA must be set to DC for best results.) Two front-panel switches are not used here; set the GATE to ANTI, and the STROBE to INTERNAL.

This device generates its output pulse by using a linear ramp generator, a capacitor charged by a stable constant-current source that is turned on by a START pulse and off by a subsequent valid STOP pulse. The slope of the ramp determines the time scale, and is selected by the front-panel range switch. The peak voltage on the capacitor is processed by the output system's Sample-and-Hold circuitry to produce a positive rectangular pulse suitable for analysis by a conventional MCA. If the module is STARTed, but receives no valid STOP pulse before expiration of the full-scale time, the logic system inhibits the output and resets the timing capacitor to zero to be ready for the next START pulse.

## PRECISION PULSE GENERATOR:

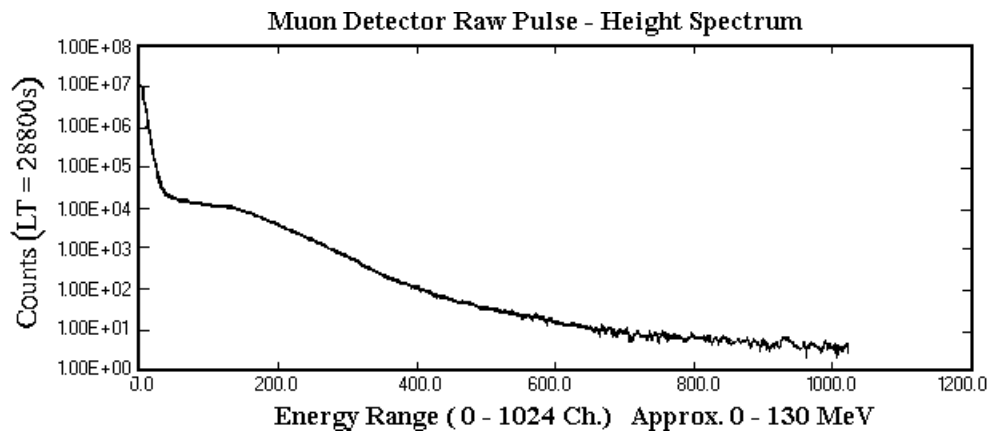
The Tennelec TC 812 Mercury-Relay Pulser is used to set the Discriminator so as to reject the low-amplitude detector pulses produced by "environmental background", principally  $^{40}\text{K}$  and  $^{228}\text{Th}$  contamination in the building structure.

## DOUBLE-PULSE GENERATOR:

The Berkeley BH-1 Tail-Pulse Generator permits investigation and verification of the performance of the various instruments. All important pulse parameters (rise time, fall time, repetition rate, time interval between pulse pairs, and output amplitude) may be adjusted. Use for determining the time calibration and performance of the TAC-MCA.

## MUON-DETECTOR PULSE-HEIGHT OUTPUT CHARACTERISTICS:

The response of the muon detector to all incident radiation from 0 to about 130 MeV is reproduced below. The electronics setup used was slightly different than that used for the experiment. The photomultiplier preamplifier was fed to a conventional wide-dynamic-range shaping amplifier (Ortec 435A) that was connected to the MCA Direct Input. (The Timing Amplifier and Linear Gate and Stretcher could not be used here because the Stretcher's 0.1 V low amplitude limit rejects the important low-energy features.) Note the very high count rate at the low-energy end extending up to a few MeV, produced by the environmental background from the building.



## EXPERIMENTAL TASKS

Obtaining valid data requires the completion of four tasks. The first entails setting amplifier gain and a Discriminator threshold level to reject signals produced by the environmental "background". The second involves setting the time scale and checking the time linearity/offset of the system. The third is the actual measurement of the Muon Lifetime. Analysis and interpretation of the data is the fourth. (It is assumed that you have already made an accurate estimate of the expected Muon count rate from the size of the detector.)

### ENERGY CALIBRATION AND THRESHOLD SETTING:

An energy calibration is established by using a moderate energy (1 MeV  $^{60}\text{Co}$ )  $\gamma$ -ray spectrum, and then using the Precision Pulse Generator to step up to the multi-MeV range. This process exhibits inherently large uncertainties and requires care to keep them reasonable. A useful pulse-height spectrum of the  $^{60}\text{Co}$  source requires that the 474 Amplifier be set to its maximum gain (250x), with a positive pulse output (Output switch to NON-INV, DIFF set to 500 ns, and INT to 20 ns). The Linear Gate and Stretcher is set for + 10 V output. The environmental background must be subtracted from the  $^{60}\text{Co}$  spectrum using the MCA's STRIP/SUM function. See Figure 11. The Stretcher's BLR signal input is set to DC. The MCA "Dead Time" will be above 20% on "background" and above 30% with the source. The spectra obtained can be best understood by careful review of your plastic-scintillator data from Experiment 12, and then considering the interactions between the  $^{60}\text{Co}$   $\gamma$ -rays with the liquid scintillator.

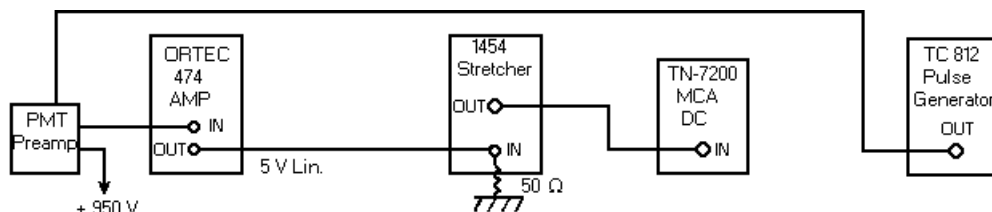


Figure 11. System for energy calibration and discriminator threshold setting.

Once a useful  $^{60}\text{Co}$  spectrum is obtained, substitute the TC-812 pulse generator output for the preamp output at the 474 Input connector. The pulser output is set to match the MCA cursor that you position at the 1 MeV point on the  $^{60}\text{Co}$  spectrum. Preset the pulser PULSE HEIGHT dial to 100 (1000 Full Scale). Use the pulser step attenuators and Calib. control (screwdriver adjustment on the front panel) to match the output to the Cursor. The Pulse Height dial will then be direct reading in MeV/major dial division. Now reset the 474 to a lower gain (2x) so that the muon/decay-electron energy range can be processed without amplifier overload. A very fast amplifier, such as the 474, does not overload cleanly and suddenly as does the Tennelec Model 214 used in Experiment 12. Instead it gradually becomes non-linear above 5 V (into 50  $\Omega$ ), with the output pulse rapidly increasing in width with

substantial inflections on the trailing edge of the output pulse. Decide the energy below which you wish pulses to be rejected, set that value on the pulser PULSE HEIGHT dial.

Reset the 474 for NEGATIVE output pulses (474 Polarity switch to INV). Connect the 474 output to the DISCrminator input (Remember that the 821 inputs are internally terminated with  $50\ \Omega$  -- DO NOT use the feed through terminator as well.) and then set the DISC. to the pulser output amplitude. Use the DISC. Rate lamp to make this adjustment - it should noticeably flicker when the adjustment is optimum. Measure the DC level at the THR jack with the Digital Multimeter. It should be slightly higher than the minimum reading of  $-300\ \text{mV}$ . The DISC setting should be high enough to reject all pulses of environmental origin (Cs, K, Th), but still low enough to pass as many as possible of the muon decays.

## TIME ADJUSTMENTS AND CALIBRATION:

Connect one of the top row of DISC. output pairs to the TAC **START** input, and one of the middle DISC. output pairs to the TAC **STOP** input. Spurious results are seen if you use the same discriminator output driver for both START and STOP signals. Select a processing time for the TAC. The usual value is  $50\ \mu\text{s}$  which unambiguously shows both the decays and the random "muon" background. There may be good reason to make a

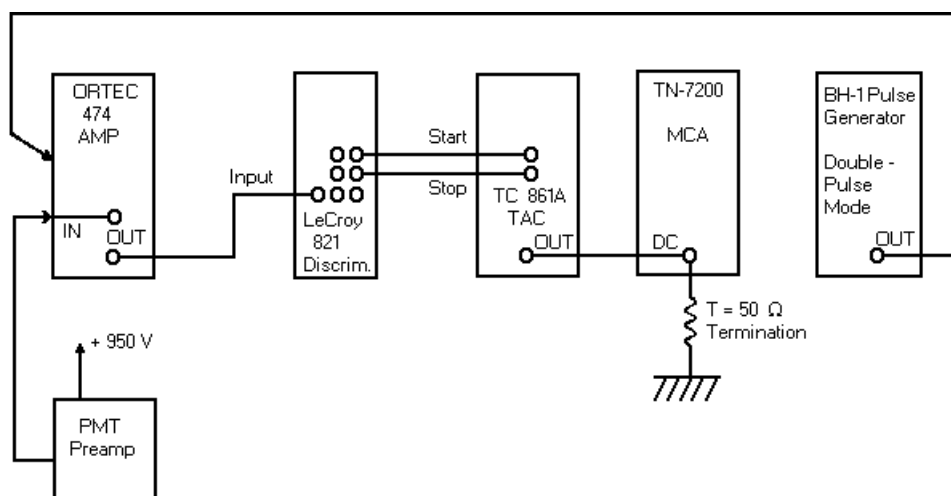


Figure 12 Electronics change for timing calibration and measurements.

second run with a different value. Shorter times will provide more data in the decay region, while longer times facilitate reaching more definite conclusions about the slope, if any, of the "background".

The Berkeley BH-1 Pulser (in Double-Pulse mode), replacing the Preamp at the 474 input, is used to verify the operation of the 474/DISC/TAC chain, calibrate the time scale, and determine the time linearity of the system. (See Figure 12.) The simplest method is to display the Disc output on the CRO and adjust the pulse spacing to exactly

match the full-scale value selected for the TAC. Accuracy will be determined by the linearity and calibration accuracy of the CRO sweep circuits, providing an uncertainty of  $\approx 1\%$ . Store the time-calibration spectrum (comb) and then determine the number of ms/channel.

When the system setup has been completed, test it (a 30 minute run will be quite adequate **IF** the count rate is correct - this rate is the most sensitive indicator.). Since the normal count rate is of the order of  $\leq 1/\text{s}$ , a full run of several hours, preferably overnight, is required to obtain adequately low statistical uncertainty in the data. Dump the data to the computer and plot it (LOG Y-scale strongly recommended). Make all necessary corrections to the data and determine the mean lifetime of the Muon, including a realistic estimate of the uncertainties in your reported values. How does it compare with the published value of  $2.197 \pm 0.001 \mu\text{s}$  [Reference (2)]? Explain any differences between this value and your measurement. Carefully consider Questions 3 and 7 below.

## QUESTIONS

1. What is the maximum energy that a muon can deposit in the  $0.21 \text{ m}^3$  detector? What is the most probable energy?
2. How would you determine the direction from which Muons enter the scintillator tank? What is the most probable direction?
3. How can you correct your measured muon lifetime for the effects of having a mixture of two types of muon?
4. What changes to the present apparatus would make it possible to determine the ratio of  $+$  to  $-$  Muons?
5. Muons detected are created in the upper atmosphere. Why isn't the lifetime measured equal to the characteristic lifetime less the time of flight from the point of creation?
6. What is the detector efficiency for detection of 1-MeV  $\gamma$ -rays? A 3-MeV  $\beta$ -ray source? A 3-MeV monoenergetic electron source? Sketch the shape of the spectra that each would produce in this detector.
7. How would you determine the energy of the stopped muons? Of the decay electrons?

## REFERENCES

- \* (1) R. B. Leighton, *Principles Of Modern Physics*, (McGraw-Hill Book Co., 1959), Chap. 20, pp. 623-632, 633-640, 680-693 .
- \* (2) E. Segre, *Nuclei And Particles*, 2nd Ed. (Benjamin/Cummings Publishing Co., 1977), pp. 730-747 .
- (3) N. Tsoulfanidis, *Measurement And Detection Of Radiation*, (McGraw-Hill Book Company, 1983), Chap.2.
- \* (4) S. Hayakawa, *Cosmic Ray Physics*, (Wiley-Interscience, 1969), Chap. 1 and 2 .
- (5) J. D. Jackson, *Classical Electrodynamics*, 2nd Ed., (John Wiley and Sons, 1974), pp. 626-637 .
- (6) B. Rossi, *High-Energy Particles*, (Prentice-Hall, Inc., 1952), Chaps. 1 and 2.
- (7) T. Ward , M. Barker, J. Breeden, K. Komisarcik, M. Pickar, D. Wark (CIT), and J. Higgins, "Laboratory study of the cosmic-ray muon lifetime," *Amer. J. Phys.*, **53** , 542 (1985).
- \* (8) Philip. R. Bevington, *Data Reduction And Error Analysis For The Physical Sciences*, (McGraw-Hill Book Company, 1969).
- (9) W. R. Leo, *Techniques for Nuclear and Particle Physics Experiments: A How-to Approach*, 2nd. rev. ed., (Springer-Verlag, 1994).
- (10) R. A. Mewaldt, "Cosmic Rays,". Caltech article published in the Macmillan Encyclopedia of Physics in 1996, courtesy of the author.

\* Primary reference. All above are available in the laboratory.



## APPENDIX

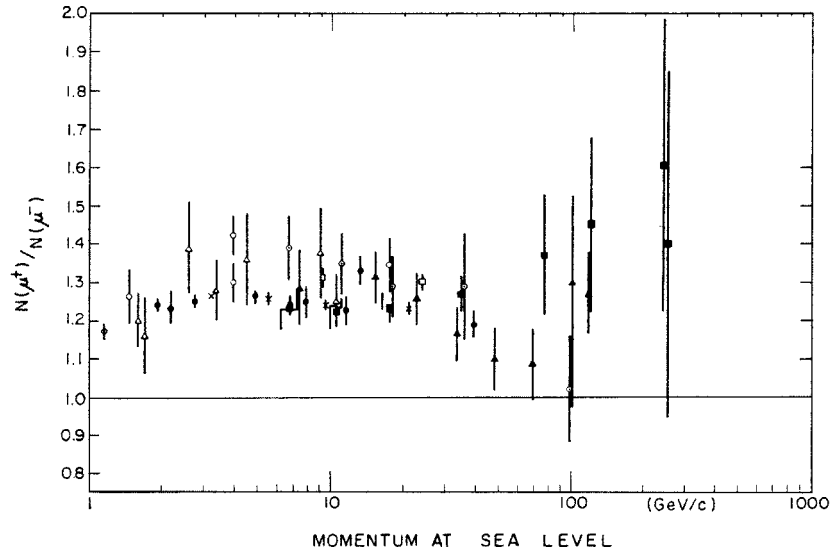


Figure A-1. Ratio of  $\mu^+$  to  $\mu^-$  vs. energy at sea level. (4), p. 380.

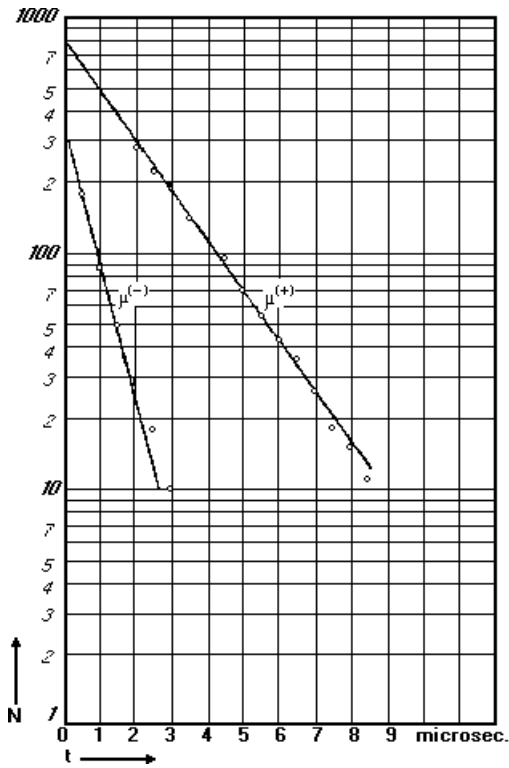


Figure A-2. Experimental data for lifetimes of  $\mu^+$  and  $\mu^-$  decaying in aluminum. (6), p. 168.